

Stronger, Fewer, & Superior: Harnessing Vision Foundation Models for Domain Generalized Semantic Segmentation

Zhixiang Wei^{1*} Lin Chen^{1,2*} Yi Jin^{1*} Xiaoxiao Ma¹ Tianle Liu¹ Pengyang Ling^{1,2} Ben Wang¹
Huaian Chen^{1†} Jinjin Zheng¹

¹ University of Science and Technology of China ² Shanghai AI Laboratory

{zhixiangwei, chlin, xiao_xiao, tleliu, lpyang27, wblzgrsn, anchen}@mail.ustc.edu.cn

{jinyi08, jjzheng}@ustc.edu.cn

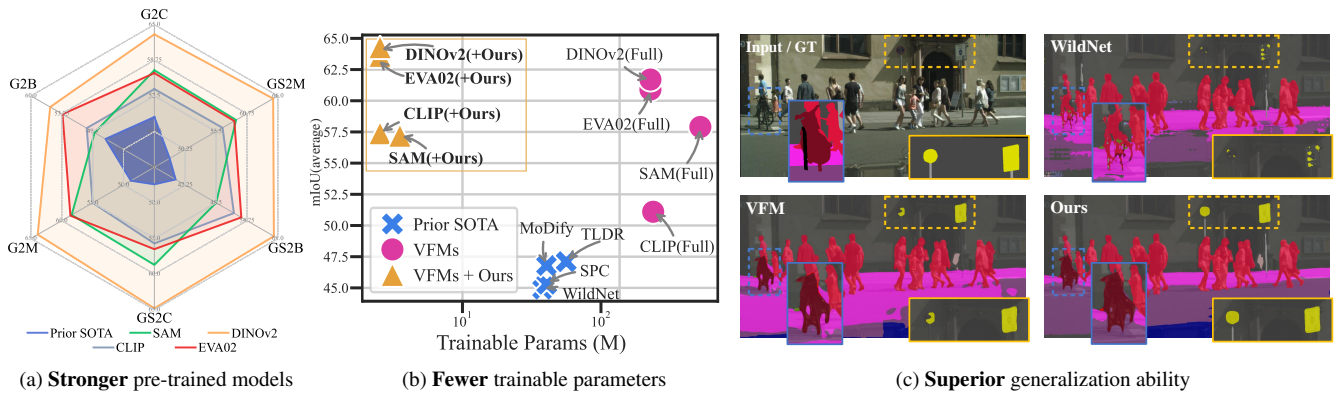


Figure 1. Vision Foundation Models (VFMs) are **stronger** pre-trained models that serve as robust backbones, effortlessly outperforming previous state-of-the-art Domain Generalized Semantic Segmentation (DGSS), as shown in (a). Yet, the extensive parameters of VFMs make them challenging to train. To address this, we introduce a robust fine-tuning approach to efficiently harness VFMs for DGSS. As illustrated in (b) and (c), the proposed methods achieve **superior** generalizability with **fewer** trainable parameters within backbones.

Abstract

In this paper, we first assess and harness various Vision Foundation Models (VFMs) in the context of Domain Generalized Semantic Segmentation (DGSS). Driven by the motivation that **Leveraging Stronger pre-trained models and Fewer trainable parameters for Superior generalizability**, we introduce a robust fine-tuning approach, namely “**Rein**”, to parameter-efficiently harness VFMs for DGSS. Built upon a set of trainable tokens, each linked to distinct instances, Rein precisely refines and forwards the feature maps from each layer to the next layer within the backbone. This process produces diverse refinements for different categories within a single image. With fewer trainable parameters, Rein efficiently fine-tunes VFMs for DGSS tasks, surprisingly surpassing full parameter fine-tuning. Extensive experiments across various settings demonstrate that Rein significantly outperforms state-of-the-art methods. Remarkably, with just an extra **1%** of trainable parameters

within the frozen backbone, Rein achieves a mIoU of **78.4%** on the Cityscapes, without accessing any real urban-scene datasets. Code is available at <https://github.com/wloves/Rein.git>.

1. Introduction

Prior works [35, 37, 39, 64, 73, 76, 82] in Domain Generalized Semantic Segmentation (DGSS) focus on improving prediction accuracy across multiple unseen domains without accessing their data, thus enabling a high generalization for real applications. Since models are fine-tuned using datasets [12, 65] that are either limited in scale or different in image style from the target domain, complex data augmentation approaches [5, 61, 83] and domain invariant feature extraction strategies [10, 59, 72, 77] have been widely explored in previous DGSS. These methods result in enhanced generalization when applied to classic backbones, e.g., VGGNet [71], MobileNetV2 [68], and ResNet [26].

In recent years, large-scale Vision Foundation Models (VFMs) like CLIP [63], MAE [27], SAM [42], EVA02 [18, 19], and DINOv2 [58] have significantly advanced the

* indicates equal contributions.

† Corresponding authors.

	Previous DGSS methods						Frozen backbone of VFMs				
Methods	GTR[61]	AdvStyle[83]	WildNet[45]	SPC[30]	PASTA[5]	TLDR[40]	CLIP-ViT-L[63]	MAE-L[27]	SAM-H[42]	EVA02-L[18]	DINOv2-L[58]
Publications	TIP21	NIPS22	CVPR22	CVPR23	ICCV23	ICCV23	ICML21	CVPR22	ICCV23	arXiv23	arXiv23
mIoU (Citys)	43.7	43.4	45.8	46.7	45.3	47.6	53.7	43.3	57.0	56.5	63.3
mIoU (BDD)	39.6	40.3	41.7	43.7	42.3	44.9	48.7	37.8	47.1	53.6	56.1
mIoU (Map)	39.1	42.0	47.1	45.5	48.6	48.8	55.0	48.0	58.4	58.6	63.9
mIoU (Average)	40.8	41.9	44.9	45.3	45.4	47.1	52.4	43.0	54.2	56.2	61.1

Table 1. Performance benchmarking of **multiple VFMs and previous DGSS methods** under the *GTAV* \rightarrow *Cityscapes (Citys)* + *BDD100K (BDD)* + *Mapillary (Map)* generalization setting. Without specialized design, frozen VFMs demonstrate **stronger** performance.

boundaries of performance in a variety of computer vision challenges. Giving the remarkable generalization of these VFMs across various unseen scenes, two intuitive questions emerge: *How do VFMs perform in the context of DGSS?* And *How to harness VFMs for DGSS?* We attempt to answer these questions as follows:

Stronger: We begin by evaluating and comparing the performance of various VFMs against existing DGSS methods. To ensure a fair comparison, we use image encoders from a variety of VFMs as the backbone for feature extraction in all cases. These backbones are coupled with the widely-used decode head, *i.e.*, Mask2Former [9], to generate semantic predictions. As illustrated in Tab. 1, while previous DGSS methods have showcased commendable results, they perform less effectively compared to frozen VFMs. This finding clearly demonstrates the powerful potential of VFMs in DGSS, outperforming traditional backbones like ResNet [26] and MobileNetV2 [68], thereby establishing VFMs as a meaningful benchmark in the field.

Fewer: Although VFMs have exhibited impressive generalization capabilities, fine-tuning them for DGSS tasks poses a challenge. The datasets [12, 65] commonly used in DGSS tasks are significantly smaller in scale compared to ImageNet [13], and fine-tuning VFMs with their huge number of trainable parameters on these datasets result in limited generalizability [36]. To address this issue, instead of the difficult task of large datasets collection, we resort to fine-tuning VFMs with fewer trainable parameters. However, most existing parameter-efficient fine-tuning strategies, which fine-tune a large-scale model with fewer trainable parameters, are primarily designed for adapting large language models [28, 29, 46, 49, 51, 80, 85] or classification networks [7, 31]. These methods are not developed for refining features for distinct instances within a single image, thereby limiting their effectiveness in DGSS contexts.

Superior: In this work, we introduce a robust and efficient fine-tuning approach, namely “Rein”. Tailored for DGSS tasks, Rein employs fewer trainable parameters to harness stronger VFMs for achieving superior generalization. At its core, Rein comprises a set of randomly initialized tokens, each directly linked to different instances. These tokens, through a dot-product operation with VFMs features, generate an attention-like similarity map. This map enables Rein to perform precise refinement tailored to

each instance within an image, significantly boosting VFMs in the context of DGSS. Moreover, to reduce the number of trainable parameters, we employ shared weights across MLPs in different layers and design our learnable tokens by multiplying two low-rank matrices. Extensive experiments on various DGSS settings demonstrate that the proposed Rein outperforms existing DGSS methods by a large margin with fewer trainable parameters. In a nutshell, the **main contributions** of this paper are as follows:

- We first assess various Vision Foundation Models (VFMs) in the context of Domain Generalized Semantic Segmentation (DGSS). Our extensive experiments in the DGSS framework highlight the impressive generalization capabilities of VFMs. The findings confirm that VFMs serve as **Stronger** backbones, thereby establishing a significant benchmark in this field.
- We present a robust fine-tuning method, namely “**Rein**”, to parameter-efficiently harness VFMs. At its core, Rein consists of a set of learnable tokens, each directly linked to instances. With deliberate design, this linkage enables Rein to refine features at an instance-level within each layer. As a result, Rein reinforces the ability of VFMs in DGSS tasks, achieving this with **Fewer** trainable parameters while preserving the pre-trained knowledge.
- Comprehensive experiments across various DGSS settings demonstrate that Rein employs **Fewer** trainable parameters to effectively leverage **Stronger** VFMs for achieving **Superior** generalizability. This performance surpasses existing DGSS methods by a large margin. Notably, Rein is designed to integrate smoothly with existing plain vision transformers, improving their generalization ability and making training more efficient.

2. Related Works

Domain Generalized Semantic Segmentation. Domain Generalized Semantic Segmentation (DGSS) focuses on enhancing model generalizability. This field involves training models on a set of source domain to enhance their performance on distinct and unseen target domain. Various approaches [6, 14, 22, 23, 30, 32–34, 48, 62, 75] have been proposed to address this issue, with methods including splitting the learned features into domain-invariant and domain-specific components [72, 77], or employing meta-learning to train more robust models [38]. A standard scenario in

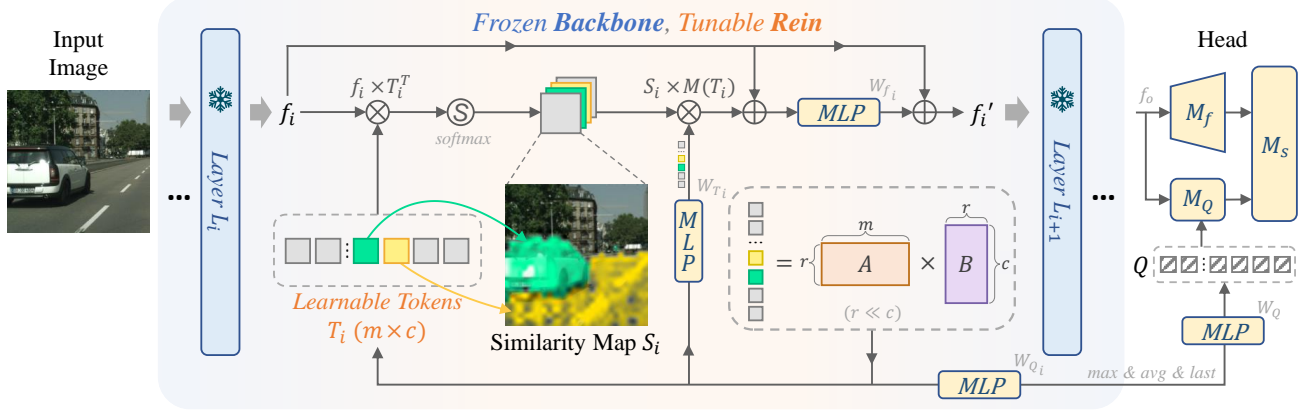


Figure 2. An overview of proposed Rein. Rein primarily consists of a collection of low-rank learnable tokens, denoted as $T = \{T_1, T_2, \dots, T_N\}$. These tokens establish direct connections to distinct instances, facilitating instance-level feature refinement. This mechanism results in the generation of an enhancement feature map $f'_i = f_i + \text{Rein}(f_i)$ for each layer within backbone. All parameters of MLPs are layer-shared to reduce the number of parameters. M_f , M_Q , and M_S are features module, queries module, and segmentation module, respectively. The notation *max & avg & last* refers to the equation Eq. (8) and Eq. (10).

Backbone	Fine-tune Method	Trainable Params*	mIoU			
			Citys	BDD	Map	Avg.
CLIP [63] (ViT-Large)	Full	304.15M	51.3	47.6	54.3	51.1
	Freeze	0.00M	53.7	48.7	55.0	52.4
	Rein	2.99M	57.1	54.7	60.5	57.4
MAE [27] (Large)	Full	330.94M	53.7	50.8	58.1	54.2
	Freeze	0.00M	43.3	37.8	48.0	43.0
	Rein	2.99M	55.0	49.3	58.6	54.3
SAM [42] (Huge)	Full	632.18M	57.6	51.7	61.5	56.9
	Freeze	0.00M	57.0	47.1	58.4	54.2
	Rein	4.51M	59.6	52.0	62.1	57.9
EVA02 [18, 19] (Large)	Full	304.24M	62.1	56.2	64.6	60.9
	Freeze	0.00M	56.5	53.6	58.6	56.2
	Rein	2.99M	65.3	60.5	64.9	63.6
DINOv2 [58] (Large)	Full	304.20M	63.7	57.4	64.2	61.7
	Freeze	0.00M	63.3	56.1	63.9	61.1
	Rein	2.99M	66.4	60.4	66.1	64.3

Table 2. Performance Comparison with the proposed **Rein** across **Multiple VFMs** as Backbones under the *GTAV* \rightarrow *Cityscapes* (*Citys*) + *BDD100K* (*BDD*) + *Mapillary* (*Map*) generalization setting. Mark * denotes trainable parameters in backbones.

DGSS is generalizing from one urban-scene dataset to another, for instance, from the synthetic GTAV [65] dataset to the real-world Cityscapes [12]. In this classic setting, certain techniques [10, 59, 60] have achieved notable performance through learning feature normalization/whitening schemes, while others [45] have improved segmentation results through feature-level style transfer and the introduction of additional data. Additionally, strong data augmentation [5, 17, 61, 83] often simply and effectively enhances model robustness. However, most of previous DGSS methods generally utilize outdated backbones like ResNet [26], VGGNet [71], MobileNetV2 [68], and ShuffleNetV2 [54], thereby leaving the efficacy of stronger Vision Foundation

Models (VFMs) in DGSS relatively unexplored.

Vision Foundation Models. The concept of a Foundation Model, initially introduced by Bommasani *et al.* [2] in the field of Natural Language Processing (NLP), defined as “the base models trained on large-scale data in a self-supervised or semi-supervised manner that can be adapted for several other downstream tasks”. While models like the ViT [15] and Swin Transformer [52] have demonstrated excellent performance, the quest for a Vision Foundation Model (VFM) similar to their NLP counterparts is ongoing. This pursuit has yielded significant advancements with the advent of models such as CLIP [63], which learn high-quality visual representation by exploring contrastive learning with large-scale image text pairs; MAE [27], utilizing a masked image modeling for learning latent image representations; SAM [42], which develops a promptable model and pre-train it on a broad dataset for segmentation task; EVA02 [18, 19], which integrates Masked Image Modeling pre-training with CLIP’s vision features; and DINOv2 [58], which is pretrained on extensive, curated datasets without explicit supervision. These VFMs have shown remarkable performance in downstream applications. Yet, a dedicated investigation into their performance in the specific context of DGSS tasks remains unexplored.

Parameter-Efficient Fine-tuning. In the realm of NLP, parameter-efficient fine-tuning (PEFT) has achieved notable success by freezing most parameters of VFMs and fine-tuning a select few. Various approaches have been developed, such as BitFit [80], which adjusts only the model’s bias terms; Prompt-tuning [46], introducing soft prompts to adapt frozen language models; Adapter-tuning [28], adding lightweight modules to each transformer layer; and notably, LoRA [29], which injects trainable rank decomposition matrices into transformer layers, yielding significant influence.

Target	ACDC[67] (test)					Cityscapes-C[56] (level-5)																
	Night	Snow	Fog	Rain	All	Blur				Noise				Digital				Weather				Avg.
						Motion	Defoc	Glass	Gauss	Gauss	Impul	Shot	Speck	Bright	Contr	Satur	JPEG	Snow	Spatt	Fog	Frost	
HGFormer	52.7	68.6	69.9	72.0	67.2	64.1	67.2	61.5	63.6	27.2	35.7	32.9	63.1	79.9	72.9	78.0	53.6	55.4	75.8	75.5	43.2	59.4
Ours	70.6	79.5	76.4	78.2	77.6	68.5	71.7	69.7	68.7	6.2	23.0	13.1	63.7	81.5	78.9	80.6	68.8	63.8	73.6	79.5	47.9	60.0

Table 3. Results on **Cityscapes** \rightarrow **ACDC (test)** and **Cityscapes-C (level-5)** datasets, utilizing a batch size of 8.

Backbone	Fine-tune Method	Trainable Params*	mIoU			
			Citys	BDD	Map	Avg.
EVA02 (Large) [18, 19]	Full	304.24M	62.1	56.2	64.6	60.9
	+AdvStyle [83]	304.24M	63.1	56.4	64.0	61.2
	+PASTA [5]	304.24M	61.8	57.1	63.6	60.8
	+GTR-LTR [61]	304.24M	59.8	57.4	63.2	60.1
	Freeze	0.00M	56.5	53.6	58.6	56.2
	+AdvStyle [83]	0.00M	51.4	51.6	56.5	53.2
	+PASTA [5]	0.00M	57.8	52.3	58.5	56.2
	+GTR-LTR [61]	0.00M	52.5	52.8	57.1	54.1
	+LoRA [29]	1.18M	55.5	52.7	58.3	55.5
	+AdaptFormer [7]	3.17M	63.7	59.9	64.2	62.6
	+VPT [31]	3.69M	62.2	57.7	62.5	60.8
	+Rein (ours)	2.99M	65.3	60.5	64.9	63.6
DINOv2 (Large) [58]	Full	304.20M	63.7	57.4	64.2	61.7
	+AdvStyle [83]	304.20M	60.8	58.0	62.5	60.4
	+PASTA [5]	304.20M	62.5	57.2	64.7	61.5
	+GTR-LTR [5]	304.20M	62.7	57.4	64.5	61.6
	Freeze	0.00M	63.3	56.1	63.9	61.1
	+AdvStyle [83]	0.00M	61.5	55.1	63.9	60.1
	+PASTA [5]	0.00M	62.1	57.2	64.5	61.3
	+GTR-LTR [5]	0.00M	60.2	57.7	62.2	60.0
	+LoRA [29]	0.79M	65.2	58.3	64.6	62.7
	+AdaptFormer [7]	3.17M	64.9	59.0	64.2	62.7
	+VPT [31]	3.69M	65.2	59.4	65.5	63.3
	+Rein (ours)	2.99M	66.4	60.4	66.1	64.3

Table 4. Performance Comparison of the proposed **Rein against other DGSS and PEFT methods** under the *GTAV* \rightarrow *Cityscapes* (*Citys*) + *BDD100K* (*BDD*) + *Mapillary* (*Map*) generalization setting. Mark * denotes trainable parameters in backbones.

The application of PEFT methods is also expanding into the field of computer vision [16, 43], with notable examples such as Visual Prompt Tuning (VPT) [31], which prepends prompts into the input sequence of transformer layers; AdaptFormer [7], replacing the MLP block in the transformer encoder with an AdaptMLP; LP-FT [43] find that fine-tuning can achieve worse accuracy than linear probing out-of-distribution; and Prompt-ICM [20], applying large-scale pre-trained models to the task of image coding for machines. Contrasting with these methods, we aim to refine feature maps for each instance within an image, thereby achieving superior performance in the realm of DGSS.

3. Methods

3.1. Preliminary

Driven by the motivation that **Leveraging Stronger pre-trained models and Fewer trainable parameters for Su-**

Source Domain	Cityscapes mIoU
GTAV	66.4
+Synthia	68.1
+UrbanSyn	78.4
+1/16 of Cityscapes Training set	82.5

Table 5. **Synthetic data + 1/16 of Citys.** \rightarrow **Citys.** val set.

prior generalizability, we choose to fine-tune VFMs with a reduced parameter set. A straightforward thought might involve a smaller decode head; however, this method merely acts as a passive receiver of feature maps from the backbone, lacking the flexibility to effectively adapt a frozen backbone for generating task-specific or scene-specific features. In contrast, we propose to embed a mechanism, named “Rein”, between the layers within the backbone. Rein actively refines and forwards the feature maps from each layer to the subsequent one. This approach allows us to more effectively utilize the powerful capabilities of VFMs, much like using rein to control a horse.

Given a pre-trained VFM with parameters Φ_M , consisting of a sequence of layers L_1, L_2, \dots, L_N , a decode head \mathcal{H} parameterized by θ_h , and the Rein strategy with parameters θ_R , the optimization objective can be written as:

$$\arg \min_{\theta_R, \theta_h} \sum_{i=1}^{N_d} \mathcal{Loss}(\mathcal{H}_{\theta_h}(\mathcal{F}_{\Phi_M, \theta_R}(x_i)), y_i), \quad (1)$$

where x_i and y_i denote the input image and its corresponding ground truth, respectively, and N_d signifies the total number of samples. $\mathcal{F}_{\Phi_M, \theta_R}$ represents the forward process of VFM after applying the Rein strategy.

3.2. Core of Rein

For simple implementation across different VFMs, we opt not to modify MLP weights at specific positions as described in the [7, 29]. Instead, our approach focuses on refining the output feature maps at each layer within the VFMs, as illustrated in Fig. 2. Precisely, for the features f_i produced by the i -th layer L_i , Rein produces enhanced feature maps for the next layer as follows:

$$\begin{aligned} f_1 &= L_1(\text{Embed}(x)) & f_1 &\in \mathbb{R}^{n \times c}, \\ f_{i+1} &= L_{i+1}(f_i + \Delta f_i) & i &= 1, 2, \dots, N-1, \\ f_{out} &= f_N + \Delta f_N, \end{aligned} \quad (2)$$

where $f'_i = f_i + \Delta f_i$ symbolizes the refined feature map, x is the input image, Embed denotes the patch embedding

layer in VFMs, n represents the number of patches, N denotes the number of layers, and c is the dimensionality of f_1, f_2, \dots, f_N . Note that the layers L_1, L_2, \dots, L_N are kept frozen, and our focus is on training an efficient module, Rein, to generate Δf_i as follows:

$$\Delta f_i = \text{Rein}(f_i) \quad \Delta f_i \in \mathbb{R}^{n \times c}, i = 1, 2, \dots, N. \quad (3)$$

In the context of DGSS, an ideal Δf_i should assist VFMs to bridge two types of gaps. The first is gap in scene between pre-training dataset and target scene, exemplified by the contrast between ImageNet [13] and urban-scene images [12, 65]. The second is task divergence between pre-training and fine-tuning, such as the differences between masked image modeling and semantic segmentation tasks.

To establish this dual bridge, Rein starts with a set of learnable tokens $T = \{T_i \in \mathbb{R}^{m \times c} \mid i \in \mathbb{N}, 1 \leq i \leq N\}$, where each token sequence T_i is randomly initialized, and m denotes the sequence length of T_i . Rein freezes the backbone and embeds knowledge learned from the fine-tuning dataset into these tokens, thereby bridging the gap in scene relative to the pre-training dataset. Moreover, considering the essential need in semantic segmentation to discern multiple instances within a single image, Rein implements an attention-inspired mechanism, which enables VFMs to make tailored adjustments to the features of distinct instances, thereby aiding VFMs in adapting to the differences between semantic segmentation and pre-training tasks. Specifically, Rein employs a dot-product operation to generate a similarity map S_i , which captures the associations between feature vectors in f_i and the tokens in T :

$$S_i = f_i \times T_i^T \quad S_i \in \mathbb{R}^{n \times m}, \quad (4)$$

where T_i represents the token sequence of the i -th layer, m indicates the number of tokens in T_i . As S quantitatively evaluates the relationships between various tokens and feature vectors, Rein can apply a softmax function to align each patch with a unique instance:

$$S_i = \text{Softmax}\left(\frac{f_i \times T_i^T}{\sqrt{c}}\right). \quad (5)$$

Leveraging the feature-to-token similarity map S_i , we can preliminarily estimates of Δf_i using the equation:

$$\Delta \bar{f}_i = S_i(:, 2 : m) \times [T_i(2 : m) \times W_{T_i} + b_{T_i}], \quad (6)$$

where W_{T_i} and b_{T_i} denote the weights and biases of a MLP, respectively. This MLP enables the transformation of T_i across different feature spaces during the computation of S_i and $\Delta \bar{f}_i$. Optionally, Rein can pre-calculate $T_i \times W_{T_i} + b_{T_i}$ to reduce inference time. The sum of S_i equals one due to the softmax function; however, this can induce unneeded changes when all features are precise. To

avoid this, $S_i(:, 2 : m)$ is designed to choose columns 2 to m of S_i , and $T_i(2 : m)$ denotes the selection of rows 2 to m of T_i . This strategic selection allows models to sidestep unnecessary adjustments by assigning a high value to the first token and subsequently discarding it. This approach allows the sum of each row in S_i to vary from 0 to 1, thus reducing the risk of inappropriate changes.

To enhance the flexibility in feature adjustment, Rein utilizes a MLP composed of W_{f_i} and b_{f_i} to produce the final feature modifications Δf_i :

$$\Delta f_i = (\Delta \bar{f}_i + f_i) \times W_{f_i} + b_{f_i}. \quad (7)$$

Benefiting from these instance-level Δf_i adjustments, Rein is capable of generating diverse modifications for various categories within a single image. The details of Rein will be explained in the next section.

3.3. Details of Rein

Linking tokens to instances. At the core of Rein, we establish an implicit yet effective linkage between tokens and instances, which has demonstrated notable performance, as detailed in Sec. 4. This connection is further reinforced by utilizing object queries, a key component in DETR[3]-style decode heads [8, 9, 81], as intermediaries. These queries are empirically proven to establish a direct association with instances. Specifically, we generate layer-wise queries Q_i from our learnable tokens T_i via linear transformation:

$$Q_i = T_i \times W_{Q_i} + b_{Q_i} \quad Q_i \in \mathbb{R}^{m \times c'}, \quad (8)$$

where W_{Q_i} and b_{Q_i} signify the weights and biases, respectively, and c' denotes the dimension of Q_i . However, due to the complexity arising from the large numbers of various layers in VFMs, transforming the diverse Q_i into a single query Q poses computational challenges. To address this, Rein computes both the maximal component $Q_{max} \in \mathbb{R}^{m \times c'}$ and the average component $Q_{avg} \in \mathbb{R}^{m \times c'}$ using the following equation:

$$\begin{aligned} Q_{max}(j, k) &= \max_{i=1,2,\dots,N} Q_i(j, k), \\ Q_{avg}(j, k) &= \frac{1}{N} \sum_{i=1}^N Q_i(j, k). \end{aligned} \quad (9)$$

Subsequently, Q is derived as:

$$Q = \text{Concat}([Q_{max}, Q_{avg}, Q_N]) \times W_Q + b_Q. \quad (10)$$

By mapping T onto Q , which subsequently links to instances, Rein achieves enhanced performance with a marginal increase in parameters.

Layer-shared MLP weights. To address the redundancy of parameters in the layer-specific MLP weights, specifically W_{T_i} in Eq. (6), W_{f_i} in Eq. (7), and W_{Q_i} in Eq. (8), which

collectively contribute to a substantial trainable parameter count, we adopt a new strategy. Since the learnable T_i is capable of producing distinct Δf_i for each layer, we design the role of the MLP to primarily perform consistent linear transformations across different feature spaces for each layer within the backbone. To this end, we employ shared MLP weights across layers as outlined in the equations:

$$\begin{aligned} [W_{T_1}, b_{T_1}] &= [W_{T_2}, b_{T_2}] = \dots = [W_{T_N}, b_{T_N}], \\ [W_{f_1}, b_{f_1}] &= [W_{f_2}, b_{f_2}] = \dots = [W_{f_N}, b_{f_N}], \\ [W_{Q_1}, b_{Q_1}] &= [W_{Q_2}, b_{Q_2}] = \dots = [W_{Q_N}, b_{Q_N}]. \end{aligned} \quad (11)$$

Low-rank token sequence. Recognizing the potential for information overlap among diverse learnable tokens, such as the high similarity between tokens representing a car’s headlight and a bicycle’s light, Rein adopts a strategy to generate a low-rank token sequence T as follows:

$$T_i = A_i \times B_i, \quad A \in \mathbb{R}^{m \times r}, B \in \mathbb{R}^{r \times c}, \quad (12)$$

where c denotes the dimension of T_i , m is the length of sequence T_i , and r represents the rank, with $r \ll c$. Here, matrices A and B are constructed as low-rank matrices. To reduce inference time, Rein can precompute and store T . By implementing this low-rank token sequence approach, Rein significantly reduces the number of parameter.

4. Experiments

4.1. Settings

Visual Foundation Models. To thoroughly assess the influence of Visual Foundation Models (VFMs) within the context of DGSS, we analyze five distinct VFMs, each with different training strategies and datasets. Our selection includes CLIP [63], a language-image pre-training model; MAE [27], known for its masked pre-training approach; SAM [42], which leverages a large-scale segmentation dataset; EVA02 [18, 19] combines CLIP with masked image modeling; and DINOv2 [58], based on self-supervised pre-training with curated dataset. For balancing precision and efficiency, we mainly employ the ViT-Large architecture for these VFMs, except SAM, which utilizes a ViT-Huge image encoder, as described in its original paper [42]. We establish two fundamental baselines for VFMs: “Full”, where we fine-tune the entire network, and “Freeze”, in which all backbone parameters are fixed, with training solely on the segmentation head. More details about VFMs and PEFT methods are available in the supplementary material.

Datasets. We evaluate VFMs and proposed methods on both real-world datasets (Cityscapes [12], BDD100K [78], Mapillary [57]) and synthetic datasets (GTAV [65], Synthia [66], UrbanSyn [24]). In detail, Cityscapes (denoted as Citys) is an autonomous driving dataset that contains 2975 training images and 500 validation images, each with the

resolution of 2048×1024 . BDD100K (shortened to BDD) and Mapillary (denoted by Map) offer 1,000 (1280×720) and 2,000 (1902×1080) validation images, respectively. GTAV, a synthetic dataset, presents 24,966 labeled images obtained from the game. Synthia, a synthetic dataset, provides 25,000 images created by photo-realistic rendering. UrbanSyn, a synthetic dataset consists of 7,539 images.

Implementation details. We utilize the MMSegmentation [11] codebase for our implementation. For superior performance, mask2former [9], a widely-used segmentation head, is integrated with various VFMs that serve as the backbone. Additional experiments involving other decode heads are detailed in the supplementary material. For the training phase, the AdamW optimizer [53] is employed, setting the learning rate at $1e-5$ for the backbone and $1e-4$ for both the decode head and the proposed Rein. Aiming to efficient training process, we utilize a configuration of 40,000 iterations with a batch size of 4, and crop images to a resolution of 512×512 . Our approach includes only basic data augmentation, following Mask2Former [9]. Thanks to our streamlined training configuration and reduced number of trainable parameters, **Rein can fine-tune models like DINOv2-Large or EVA02-Large on a single RTX 3090Ti GPU within 12 hours** for superior generalization ability.

4.2. Comparison with State-of-The-Art Methods

In this section, we comprehensively evaluate Rein over five datasets within three generalization settings: $GTAV \rightarrow Citys + BDD + Map$, $GTAV + Synthia \rightarrow Citys + BDD + Map$, and $Citys \rightarrow BDD + Map$. Rein is benchmarked against state-of-the-art (SOTA) methods, which can be classified into two groups, including domain generalized semantic segmentation (DGSS) methods [5, 10, 14, 30, 38, 45, 59, 61, 62, 74, 79, 83], and parameter-efficient fine-tuning (PEFT) approaches [7, 29, 31].

Investigation of various VFMs. Our analysis of VFMs and proposed Rein in the $GTAV \rightarrow Citys + BDD + Map$ setting is presented in Tables 1 and 2. In this setup, models are fine-tuned using GTAV and evaluated on Cityscapes, BDD100K, and Mapillary. Note that, due to the fixed and relatively small number of trainable parameters in the decode head (20.6M), the count of trainable parameters presented in the tables are focused solely on the backbone and the PEFT module. Our results, as detailed in Table 1, indicate that frozen VFMs significantly outperform previous DGSS methods without specialized design. Moreover, as shown in Table 2, VFMs with full parameter fine-tuning exhibit enhanced performance relative to their frozen counterparts. Remarkably, Rein achieves even superior generalization capabilities, surpassing the full parameter fine-tuning with merely an extra 1% of trainable parameters compared to the original backbone. Visual samples for qualitative comparison are given in Fig. 3.

Backbone	Fine-tune Method	Trainable Params*	road	side.	build.	wall	fence	pole	light	sign	vege	terr.	sky	pers.	rider	car	truck	bus	train	moto.	bicy.	mIoU
EVA02 (Large) [18, 19]	Full	304.24M	89.3	46.9	89.9	47.7	45.6	50.1	56.8	42.2	88.8	48.4	89.9	75.8	49.0	90.5	45.3	69.2	55.9	44.4	55.1	62.2
	Freeze	0.00M	93.1	52.7	88.0	47.4	31.1	41.7	46.0	39.6	85.7	41.4	89.5	67.5	39.7	89.0	47.0	72.8	46.3	19.2	35.2	56.5
	Rein-core	52.84M	91.1	53.8	90.0	50.3	47.7	46.6	56.4	42.9	87.8	44.2	90.4	73.5	44.2	91.8	58.1	77.2	57.3	43.4	57.3	63.4
	+ Rein-link	59.33M	90.9	48.5	90.0	52.6	49.4	49.1	57.2	39.8	88.9	46.5	90.5	74.4	44.0	91.0	52.3	80.7	67.3	44.3	60.3	64.1
	+ Rein-share	5.02M	92.7	54.3	90.0	51.8	48.6	48.8	55.3	45.0	88.9	46.7	89.8	73.7	43.3	90.6	49.5	81.1	69.6	41.7	50.2	63.4
	+ Rein-lora	2.99M	91.7	51.8	90.1	52.8	48.4	48.2	56.0	42.0	89.1	44.1	90.2	74.2	47.0	91.1	54.5	84.1	78.9	47.2	59.4	65.3
DINOv2 (Large) [58]	Full	304.20M	89.0	44.5	89.6	51.1	46.4	49.2	60.0	38.9	89.1	47.5	91.7	75.8	48.2	91.7	52.5	82.9	81.0	30.4	49.9	63.7
	Freeze	0.00M	92.1	55.2	90.2	57.2	48.5	49.5	56.7	47.7	89.3	47.8	91.1	74.2	46.7	92.2	62.6	77.5	47.7	29.6	47.2	61.1
	Rein-core	52.84M	92.4	57.8	90.6	56.8	50.7	50.5	57.5	44.8	89.8	47.0	91.1	75.9	47.2	91.9	60.1	80.3	59.8	37.9	52.3	64.9
	+ Rein-link	59.33M	91.2	55.5	90.6	55.6	52.5	51.1	59.7	45.1	89.8	47.1	91.1	75.8	47.1	92.6	64.6	82.2	65.5	40.4	52.7	65.8
	+ Rein-share	5.02M	93.5	61.2	90.7	57.7	53.2	52.4	58.0	50.1	89.7	49.9	90.7	74.8	45.0	91.7	58.5	80.1	66.3	36.9	50.7	65.8
	+ Rein-lora	2.99M	92.4	59.1	90.7	58.3	53.7	51.8	58.2	46.4	89.8	49.4	90.8	73.9	43.3	92.3	64.3	81.6	70.9	40.4	54.0	66.4

Table 6. Ablation Study about Rein under *Cityscapes* \rightarrow *BDD100K* generalization in terms of mIoU. Components are sequentially incorporated. To better illustrate the gains contributed by each component, we employ varying shades of yellow to demonstrate the relative performance of the Freeze and Rein methods. The best results across all methods are **highlighted**.

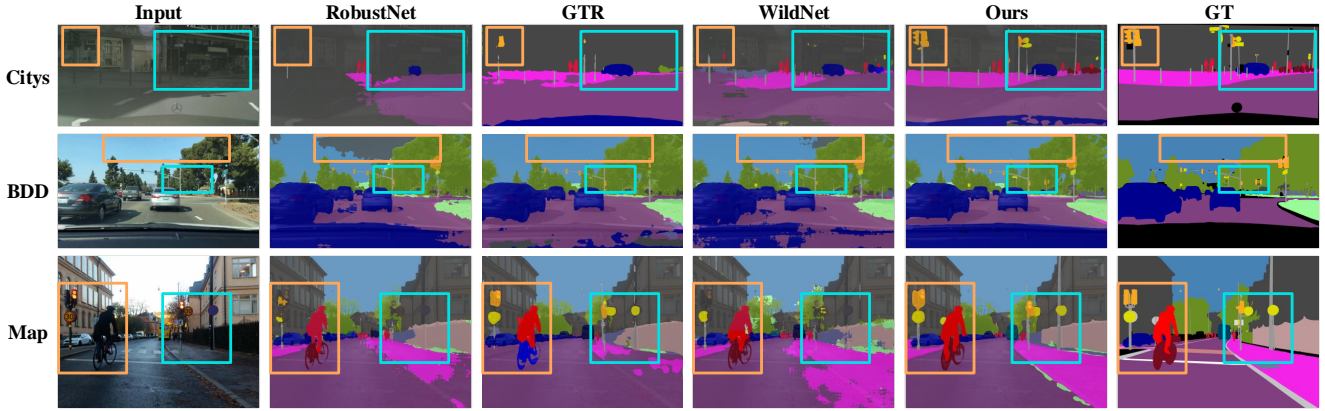


Figure 3. Qualitative Comparison under *GTAV* \rightarrow *Cityscapes* (*Citys*) + *BDD100K* (*BDD*) + *Mapillary* (*Map*) generalization setting.

Comparing Rein with SOTA. We conduct a comprehensive performance comparison of the proposed **Rein** against existing **DGSS** and **PEFT** methods under the *GTAV* \rightarrow *Citys* + *BDD* + *Map* setting, as detailed in Table 4. Owing to the robust feature extraction capabilities inherent in VFMs, DGSS methods, which typically enhance generalizability through strong data augmentation or consistency constraints, (e.g., AdvStyle, PASTA, and GTR), do not exhibit significant performance improvement. On the other hand, PEFT methods have demonstrated notable advancements. For instance, AdaptFormer outperforms the “Freeze” baseline using EVA02 as the backbone, while VPT shows improved performance over “Full” with DINOv2. Employing the same backbones (DINOv2 and EVA02), proposed Rein achieves superior performance and surpass previous DGSS and PEFT methods.

Real-to-Real generalization of Rein. The generalization from one real-world dataset to others is pivotal for practical applications in the field. To this end, we conduct experiments under the *Citys* \rightarrow *ACDC*, *Citys* \rightarrow *Cityscapes-C*, and *Citys* \rightarrow *BDD* + *Map* generalization setting. As shown in Table 3 and 7, Rein, when coupled with the DINOv2-Large, demonstrates superior performance across all datasets. This underscores the effectiveness of Rein in generalizing to diverse real-world scenarios.

Synthetic-to-real generalization of Rein. As Tab. 11 illustrates, trained on **synthetic** *UrbanSyn*+*GTAV*+*Synthia* datasets, Rein achieved a **78.4% mIoU** on the *Cityscapes* validation set. Further improvement is possible with additional synthetic data and higher-quality images generated by diffusion models, like [1]. This result can also be a valuable pre-trained weight for data-efficient training, **reaching an 82.5% mIoU with 1/16 of Cityscapes training set**. This is a significant performance for semi-supervised semantic segmentation.

More backbones. We extend our analysis to integrating Rein with Convolutional Networks, such as ResNet and ConvNeXt, and smaller scale architectures like DINOv2-S/B. As shown in Table 8, our findings reveal that Rein exhibits remarkable performance with diverse backbones.

4.3. Ablation Studies and Analysis

We conduct extensive ablation studies within two settings: *GTAV* \rightarrow *Citys* and *GTAV* \rightarrow *Citys* + *BDD* + *Map*.

Analysis of the key components. Table 6 is dedicated to thoroughly examining the effectiveness of each component within Rein. In the *GTAV* \rightarrow *Citys* generalization setting, we sequentially incorporate different components of Rein and assess their impact. Interestingly, we observe that the “Freeze” occasionally exhibit better recognition for specific

Methods	Backbone	Trainable Parameters*	mIoU		
			BDD	Map	Avg.
IBN [59]	ResNet50 [26]	23.58M	48.6	57.0	52.8
DRPC [79]	ResNet50 [26]	23.58M	49.9	56.3	53.1
GTR [61]	ResNet50 [26]	23.58M	50.8	57.2	54.0
SAN-SAW [62]	ResNet50 [26]	23.58M	53.0	59.8	56.4
WildNet [45]	ResNet101 [26]	42.62M	50.9	58.8	54.9
HGFormer [14]	Swin-L [52]	196.03M	61.5	72.1	66.8
Freeze	EVA02-L [18]	0.00M	57.8	63.8	60.8
Rein (Ours)	EVA02-L [18]	2.99M	64.1	69.5	66.8
Freeze	DINOv2-L [58]	0.00M	63.4	69.7	66.7
Rein (Ours)	DINOv2-L [58]	2.99M	65.0	72.3	68.7

Table 7. Performance Comparison of the **Rein against other DGSS methods** under *Cityscapes* \rightarrow *BDD100K (BDD) + Mapillary (Map)* generalization. The best results are **highlighted**.

Avg. mIoU	ResNet	ResNet	ConvNeXt	DINOv2	DINOv2
	(50)	(101)	(Large)	(S)	(B)
Full	38.9	46.1	52.2	51.8	56.7
Ours	46.6	46.3	55.5	55.7	59.1

Table 8. Results for **ConvNets and smaller backbones**.

categories, e.g., ‘road, sidewalk’, compared to the “Full”. This suggests that VFMs lose some pre-training knowledge during fine-tuning, and “Freeze” helps to prevent. Similarly, our methods mitigate this knowledge forgetting. Furthermore, our methods show improved recognition capabilities for the majority of the 19 categories. For example, in recognizing ‘wall, motorcycle, bicycle’, our approach significantly outperforms both the “Full” and “Freeze” baselines.

Overall, “Rein-core” boosts the average performance across 19 classes. Furthermore, “Rein-link” further boosts accuracy for certain objects, including ‘car, bus, train, motorcycle’, especially for DINOv2. Employing layer-shared MLP weights and low-rank token sequence efficiently reduces the number of trainable parameters and positively influences the performance of the model.

Study on token length m . The core component of Rein is learnable tokens $T \in \mathbb{R}^{m \times c}$. We explored various lengths m for the token sequence, ranging from 25 to 200. As demonstrated in Fig. 4, models with $m = 100$ and $m = 150$ both achieve a strong mIoU of 64.3%. We ultimately selected $m = 100$ as the most suitable parameter.

Study on rank r . As shown in Table 12, we turn attention to the effect of rank r on model performance. With DINOv2 as the backbone, the optimal results are observed at $r = 16$ and $r = 32$. Consequently, unlike LoRA [29], we opt for a comparatively higher value of $r = 16$ for our model.

Speed, memory, and storage. For practical applications, training speed, GPU memory usage, and model storage requirements are crucial. As shown in Table 13, compared to “Full” baseline, proposed Rein improves training speed and reduces GPU memory usage. A significant advantage of Rein is that models trained under different settings can share the same backbone parameters. This means that for switch

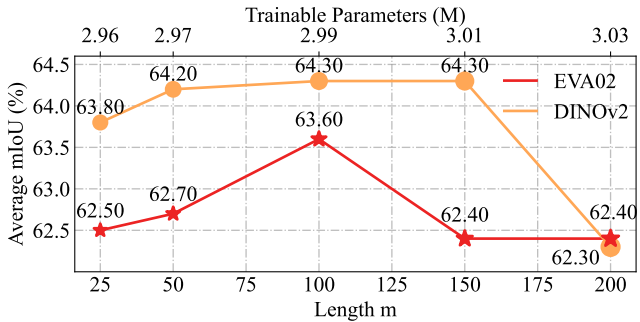


Figure 4. Ablation study on token length m .

Rank r Params		4	8	16	32	64
		2.67M	2.77M	2.99M	3.42M	4.28M
DINOv2 (Large) [58]	Citys	65.8	66.1	66.4	66.1	66.4
	BDD	60.2	60.3	60.4	60.7	61.0
	Map	65.2	65.1	66.1	65.9	65.0
	Avg.	63.7	63.9	64.3	64.3	64.1

Table 9. Ablation study on lora dim r .

VFMs	Method	Training Time	GPU Memory	Storage
DINOv2 (Large)	Full	11.2 h	14.7 GB	1.22 GB
	Rein	9.5 h	10.0 GB	1.23 GB

Table 10. Training Time, GPU Memory, and Storage.

in diverse tasks and settings, we can only store and swap the rein weights (0.01GB) and head weights (0.08GB), rather than all parameters.

5. Conclusions

In this paper, we assess and harness Vision Foundation Models (VFMs) in the context of DGSS. Driven by the motivation that **Leveraging Stronger pre-trained models and Fewer trainable parameters for Superior generalizability**, we first investigate the performance of VFMs under diverse DGSS settings. Subsequently, we introduce a robust fine-tuning approach, namely **Rein**, to parameter-efficiently harness VFMs for DGSS. With a fewer trainable parameters, Rein significantly enhance generalizability of VFMs, outperforming SOTA methods by a large margin. Rein can be seamlessly integrated as a plug-and-play adapter for existing VFMs, improving generalization with efficient training. Extensive experiments demonstrate the substantial potential of VFMs in the DGSS field, validating the effectiveness of proposed Rein in harnessing VFMs for DGSS.

6. Acknowledgements

This work was supported in part by the Anhui Provincial Key Research and Development Plan 202304a05020072, in part by the Postdoctoral Fellowship Program of CPS-FGZB20230713, and in part by the National Natural Science Foundation of China under Grant 61727809.

Stronger, Fewer, & Superior: Harnessing Vision Foundation Models for Domain Generalized Semantic Segmentation

Supplementary Material

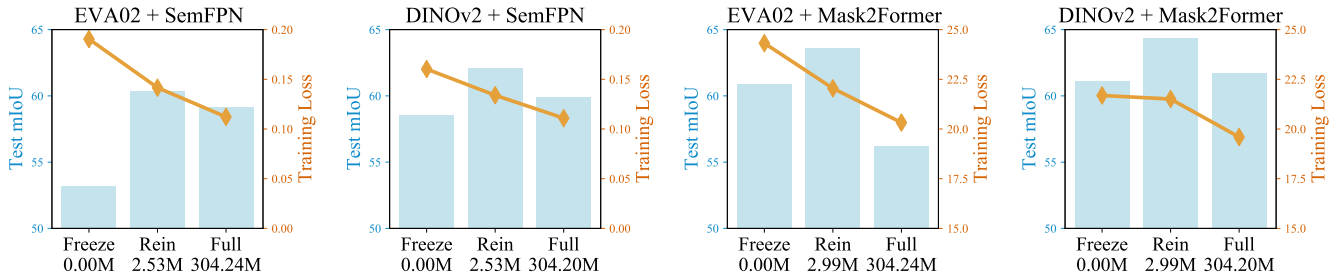


Figure 5. The curves of training loss and test metrics display consistent trends across different VFMs and decode heads: intuitively, as trainable parameters increase from $0.00M$ (*Freeze*) \rightarrow $2.53M$ (*Rein*) \rightarrow $304.24M$ (*Full*), the training loss monotonically decreases, indicating that a greater number of trainable parameters indeed better fit the training dataset. However, the test metrics on the target dataset initially rise and then fall, forming an inverted U-shape. This pattern suggests that the “Full” baseline overfits the training data, leading to diminished test performance. These findings are aligned with our motivation that **Leveraging Stronger pre-trained models and Fewer trainable parameters for Superior generalizability**. The blue bar charts in the figure represent the average mIoU tested on the Cityscapes, BDD100K, and Mapillary datasets, while the yellow line denotes the training loss during fine-tuning on GTAV dataset.

7. Fewer Trainable Parameters

Classical neural network theory [21, 25] points out that as model capacity increases, the empirical risk (or training risk) monotonically decreases, indicating an improved fit to training data. Conversely, the true risk (or test risk) typically exhibits a “U-shaped” curve, initially decreasing and then increasing, a phenomenon known as overfitting. From a modern viewpoint, the scaling law [36] suggests that on a smaller fixed dataset, performance stops to improve as model parameters increase, leading to overfitting.

In the majority of general tasks, the practice of early-stopping, based on evaluation data, can partly mitigate overfitting. However, in the field of domain generalization, the unknown test data distribution makes acquiring a valid evaluation dataset unavailable. Moreover, fine-tuning datasets are often smaller compared to ImageNet [13] or LVD-142M [58]. Hence, employing fewer trainable parameters emerges as a strategic approach to mitigate overfitting.

In our main paper, extensive experiments comprehensively demonstrate Rein’s pivotal role in enhancing the generalization capabilities of VFMs. This enhancement may be attributed to two factors: 1) Rein’s improved fitting capability for VFMs, ensuring better alignment with training data; 2) Rein’s reduction of overfitting in VFMs during fine-tuning on smaller datasets, thus exhibiting enhanced generalization in testing. To delve into this, we analyze and compare the average training loss in the final 1000 iterations of the fine-tuning phase and their corresponding test metrics for various VFMs and decode heads.

Fig. 5 showcases a consistent trend across four differ-

ent configurations. As trainable parameters increase from $0.00M$ (*Freeze*) \rightarrow $2.53M$ (*Rein*) \rightarrow $304.24M$ (*Full*), the training loss monotonically decreases. However, the test metrics on the target dataset peak with Rein, which employs 2.53 million parameters and incurs a sub-optimal training loss. In contrast, the “Full” baseline, despite recording the lowest training loss, only achieves sub-optimal test performance, a clear indicator of overfitting when compared to other setups. This observation aligns with the conclusions in [21, 36], supporting our observation that **leveraging Stronger pre-trained models and Fewer trainable parameters can lead to Superior generalizability**.

Source Domain	Cityscapes mIoU
GTAV	66.4
+Synthia	68.1
+UrbanSyn	78.4
+1/16 of Cityscapes Training set	82.5

Table 11. Results on Cityscapes validation set.

8. Value of synthetic data

As Tab. 11 illustrates, trained on synthetic *UrbanSyn* [24]+*GTA*+*Synthia* datasets, Rein achieved a **78.4% mIoU** on the Cityscapes validation set. Further improvement is possible with additional synthetic data and higher-quality images generated by diffusion models, like [1]. This result can also be a valuable pre-trained weight for data-efficient training, reaching an 82.5% mIoU with 1/16 of

Rank r		4	8	16	32	64
Params		2.67M	2.77M	2.99M	3.42M	4.28M
EVA02 (Large) [18]	Citys	62.6	63.5	65.3	63.8	63.4
	BDD	58.5	58.9	60.5	60.5	60.2
	Map	63.7	63.8	64.9	64.5	64.3
	Avg.	61.6	62.1	63.6	62.9	62.7

Table 12. Ablation study on lora dim r .

VFM	Method	Training Time	GPU Memory	Storage
EVA02 (Large)	Full	11.8 h	15.9 GB	1.22 GB
	Rein	10.5 h	12.5 GB	1.23 GB

Table 13. Training Time, GPU Memory, and Storage.

Cityscapes training set. This is a significant performance for semi-supervised semantic segmentation.

9. Ablation on decode head

Our experiments on Rein employ the Mask2Former [9] decode head, which shares structures or core concepts with numerous methods in dense prediction tasks [3, 8, 47, 55, 81]. The universality of Mask2Former highlights the significance of our findings for a range of segmentation tasks, including instance and panoptic segmentation. Furthermore, to demonstrate Rein’s effectiveness in enhancing backbone generalization and its robustness across various decode heads, we conduct supplementary experiments using the popular SemFPN decode head [41], in the $GTAV \rightarrow Cityscapes + BDD100K + Mapillary$ setting.

As shown in Table 14, Rein surpasses the “Full” and “Freeze” baselines, employing 2.53 million trainable parameters within the backbone, while the SemFPN decode head comprises 1.63 million parameters. Owing to the absence of object queries in SemFPN, the “linking tokens to instance” mechanism, described in Sec.3.3, is not utilized, resulting in a reduction of Rein’s trainable parameters from 2.99 million to 2.53 million. When compared to the complete Rein configuration using the Mask2Former, using SemFPN achieves sub-optimal performance, evident in the 64.3% mIoU reported in Table 2 and 62.1% mIoU in Table 9, both implemented with DINOv2-Large. As shown in Table 15, the Mask2Former brings the 11.7% mIoU for ResNet101. These findings guide our decision to focus on experiments involving Mask2Former in the main paper.

10. Ablation on EVA02

Study on rank r As shown in Table 12, with EVA02 as the backbone, the optimal results are observed at $r = 16$.

Speed, memory, and storage. As shown in Table 13, compared to “Full” baseline, proposed Rein improves training speed and reduces GPU memory usage.

Backbone	Fine-tune Method	Trainable Params*	mIoU			
			Citys	BDD	Map	Avg.
EVA02 [18, 19] (Large)	Full	304.24M	58.5	56.9	62.0	59.1
	Freeze	0.00M	54.1	51.2	54.3	53.2
	Rein	2.53M	61.4	58.5	62.0	60.7
DINOv2 [58] (Large)	Full	304.20M	61.2	55.9	62.5	59.9
	Freeze	0.00M	58.9	56.4	60.3	58.5
	Rein	2.53M	63.6	59.0	63.7	62.1

Table 14. Performance Comparison with the proposed **Rein with SemFPN** [41] as Backbones under the $GTAV \rightarrow Cityscapes$ ($Citys$) + $BDD100K$ (BDD) + $Mapillary$ (Map) generalization setting. Models are fine-tuned on GTAV and tested on Cityscapes, BDD100K and Mapillary. The best results are **highlighted**. * denotes trainable parameters in backbones.

Backbone	Decoder	Tune	mIoU
ResNet101 [45]	DeeplabV3plus	Full	34.4
ResNet101	Mask2Former	Full	46.1
DINOv2	Mask2Former	Full	61.7
DINOv2	Mask2Former	Ours	64.3

Table 15. Results on $GTAV \rightarrow Citys + BDD + Map$. Metrics for first line are from Wildnet.

Methods	Publication	mIoU			
		Citys	BDD	Map	Avg.
RobustNet [10]	CVPR 21	37.7	34.1	38.5	36.8
PintheMem [38]	CVPR 22	44.5	38.1	42.7	41.8
SAN-SAW [62]	CVPR 22	42.1	37.7	42.9	40.9
WildNet [45]	CVPR 22	43.7	39.9	43.3	42.3
DIGA [74]	CVPR 23	46.4	33.9	43.5	41.3
SPC [30]	CVPR 23	46.4	43.2	48.2	45.9
EVA02 - Frozen [18, 19]	arXiv 23	55.8	55.1	59.1	56.7
EVA02 + Rein	-	63.5	60.7	63.9	62.7
DINOv2 - Frozen [58]	arXiv 23	64.8	60.2	65.2	63.4
DINOv2 + Rein	-	68.1	60.5	67.1	65.2

Table 16. Performance Comparison of the proposed **Rein against other DGSS methods** under $GTAV + Synthia \rightarrow Cityscapes$ ($Citys$) + $BDD100K$ (BDD) + $Mapillary$ (Map) generalization.

11. Multi-source generalization.

In this part, we compare Rein against other DGSS methods under $GTAV + Synthia \rightarrow Citys + BDD + Map$ setting, in which networks are fine-tuned using both GTAV and Synthia datasets, and tested on Cityscapes, BDD100K, and Mapillary. As shown in Table 16, we report the performance of Rein employing two VFMs, EVA02 and DINOv2. Our results demonstrate that Rein significantly surpasses existing DGSS methods by a large margin in average mIoU (from 45.9% to 65.2%).

12. More details about VFMs

CLIP. In our study, we utilize the ViT-Large architecture, setting the patch size to 16×16 . Each layer of this ar-

chitecture outputs features with a dimensionality of 1024, making use of the pre-trained weights from the foundational work [63]. Our model undergoes a pre-training phase through contrastive learning, employing publicly available image-caption data. This data is compiled through a blend of web crawling from select websites and integrating widely-used, existing image datasets. For the model’s pre-trained weights, which have a patch size of 14×14 and an original pre-training image size of 224×224 , we adopt bilinear interpolation to upscale the positional embeddings to a length of 1024. Moreover, trilinear interpolation is utilized to enlarge the kernel size of the patch embed layer to 16×16 . Our model comprises 24 layers, and the features extracted from the 7th, 11th, 15th, and 23rd layers (counting from the zeroth layer) are subsequently channeled into the decoding head.

MAE. Employing the ViT-Large architecture, our model outputs features from each layer with a dimensionality of 1024, maintaining a patch size of 16×16 . This model capitalizes on the pre-trained weights as delineated in the original work [27], and it undergoes self-supervised training using masked image modeling on ImageNet-1K. The architecture is composed of 24 layers, directing features from the 7th, 11th, 15th, and 23rd layers directly into the decoding head.

SAM. Aligning with the methodology described in the foundational paper [42], we employ the ViT-Huge architecture as our image encoder, making use of pre-trained weights that were trained on SA-1B [42] for a promptable segmentation task. The patch size of this model is set to 16×16 , and each layer is designed to output features with a dimensionality of 1280, summing up to a total of 32 layers. The positional embeddings of the model are upsampled to a length of 1024 via bicubic interpolation. From this model, we extract features from the 7th, 15th, 23rd, and 31st layers and feed them into the decoder.

EVA02. In our approach, we adopt the largest scale configuration, EVA02-L, as our structural backbone, as suggested in the paper [18]. This particular model configuration determines its patch size as 16, with each layer producing feature maps of 1024 dimensions, across a total of 24 layers. EVA02 undergoes training through a combination of CLIP and Masked Image Modeling techniques on an aggregated dataset that includes IN-21K [13], CC12M [4], CC3M [70], COCO [50], ADE20K [84], Object365 [69], and OpenImages [44]. Mirroring the approach used in previous models, we upscale the positional embeddings to 1024 through bilinear interpolation, and the patch embed layer’s convolutional kernel size is augmented to 16×16 via bicubic interpolation. Features from the 7th, 11th, 15th, and 23rd layers are then processed through the decode head.

DINOv2. Our choice of backbone for this study is DINOv2-L, which has been distilled from DINOv2-g. As

noted in the original documentation, DINOv2-L occasionally surpasses the performance of DINOv2-g [58]. Sharing the same patch size, dimensionality, and layer count as EVA02-L, we apply equivalent processing to both the positional embeddings and patch embed layer of DINOv2-L. The features extracted from the 7th, 11th, 15th, and 23rd layers are subsequently fed into the decode head. DINOv2 is originally pretrained in a self-supervised fashion on the LVD-142M [58] dataset, following the procedures outlined in its respective paper.

VPT, LoRA, and AdaptFormer. Based on extensive experimentation, we have optimized the implementation of PEFT methods for DINOv2, utilizing configurations that enhance performance. These methods include: 1) VPT: It is deep and has 150 tokens. 2) LoRA: Applied to the query and value MLP components, LoRA is configured with a rank of 8. Additionally, it incorporates a minimal dropout rate of 0.1%. 3) AdaptFormer: This method employs a bottleneck design with a width of 64, initialized using LoRA. Notably, it omits layer normalization.

13. Algorithm of Proposed Rein

Algorithm 1 outlines the training procedure for Rein, wherein the weights conform to the constraints specified in Eq. (11). In this context, the variable c represents the number of channels in the feature maps of model \mathcal{M} , N denotes the total number of layers within \mathcal{M} , T indicates the overall number of training iterations, and r is defined as a hyperparameter that is considerably smaller than c .

14. Qualitative Results and Future works

In this section, we showcase our prediction results across various datasets, including Cityscapes, BDD100K, and Mapillary, as depicted in Fig.6, Fig.8, and Fig.7. All models are trained on the GTAV dataset without any fine-tuning on real-world urban-scene datasets. Our method outshines other approaches in accuracy, especially in categories like traffic signs, bicycles, traffic lights, sidewalks, roads, and trucks, demonstrating high precision for both large objects and smaller targets. Notably, despite not specifically optimizing for night-time segmentation, Rein’s performance during night conditions is surprisingly high, almost akin to daytime performance, as illustrated in Fig.6.

With the rapid development of generative models research, we anticipate that our work could leverage high-quality generated samples to approach the performance of models trained with supervision on real datasets. Furthermore, we are prepared to investigate how VFMs can enhance the performance of semantic segmentation models trained on real datasets under various adverse weather conditions or on special road types. Finally, further exploration is necessary to investigate how Rein can be extended to

Algorithm 1: Training process of Rein.

Input: A sequence of input data and corresponding labels $\{(x_i, y_i) \mid t \in \mathbb{N}, 1 \leq i \leq N_d\}$; Pre-trained Vision Foundation Model \mathcal{M} , consisting of a patch embed layer L_{emb} , and layers L_1, L_2, \dots, L_N ; a decode head \mathcal{H} ; and a proposed module Rein \mathcal{R} . The module Rein comprises the following matrices and vectors, initialized as specified:

$$\begin{aligned} A_i &\in \mathbb{R}^{m \times r}, & \text{uniformly initialized,} \\ B_i &\in \mathbb{R}^{r \times c}, & \text{uniformly initialized,} \\ W_{T_i} &\in \mathbb{R}^{c \times c}, & \text{uniformly initialized,} \\ W_{f_i} &\in \mathbb{R}^{c \times c}, & \text{initialized to zero,} \\ W_{Q_i} &\in \mathbb{R}^{c \times c'}, & \text{uniformly initialized,} \\ b_{T_i} &\in \mathbb{R}^c, & \text{initialized to zero,} \\ b_{f_i} &\in \mathbb{R}^c, & \text{initialized to zero,} \\ b_{Q_i} &\in \mathbb{R}^{c'}, & \text{initialized to zero,} \end{aligned}$$

for each $i \in \mathbb{N}, 1 \leq i \leq N$. Additionally,
 $W_Q \in \mathbb{R}^{3c' \times c'}$ is uniformly initialized, and
 $b_Q \in \mathbb{R}^{c'}$ is initialized to zero.

Output: The optimized \mathcal{H} and \mathcal{R} .

for $t \leftarrow 1$ **to** T **do**

 Get batch data: (x, y)

$f_0 = L_{\text{emb}}(x)$

for $i \leftarrow 1$ **to** N **do**

$f_i = L_i(f_{i-1})$

$T_i = A_i \times B_i$

$S_i = \text{Softmax}(\frac{f_i \times T_i^T}{\sqrt{c}})$

$\Delta \bar{f}_i = S_i(:, 2 : m) \times [T_i(2 : m) \times W_{T_i} + b_{T_i}]$

$\Delta f_i = (\Delta \bar{f}_i + f_i) \times W_{f_i} + b_{f_i}$

$Q_i = T_i \times W_{Q_i} + b_{Q_i}$

$f_i = f_i + \Delta f_i$

$\mathbb{F}_t \subseteq \{f_0, f_1, \dots, f_N\}$

 Calculate Q_{max} and Q_{avg} by Eq. (9)

$Q = \text{Concat}([Q_{\text{max}}, Q_{\text{avg}}, Q_N]) \times W_Q + b_Q$

$\bar{y}_t = \mathcal{H}(\mathbb{F}_t, Q)$

 Optimize \mathcal{H} and \mathcal{R} by $\text{Loss}(\bar{y}, y)$

tasks such as instance segmentation, panoptic segmentation, open-vocabulary segmentation, and even object detection.



Figure 6. Prediction results of DINOv2+Rein on the BDD100K validation set. The model is fine-tuned exclusively on the GTAV dataset, without access to any real-world urban-scene datasets.

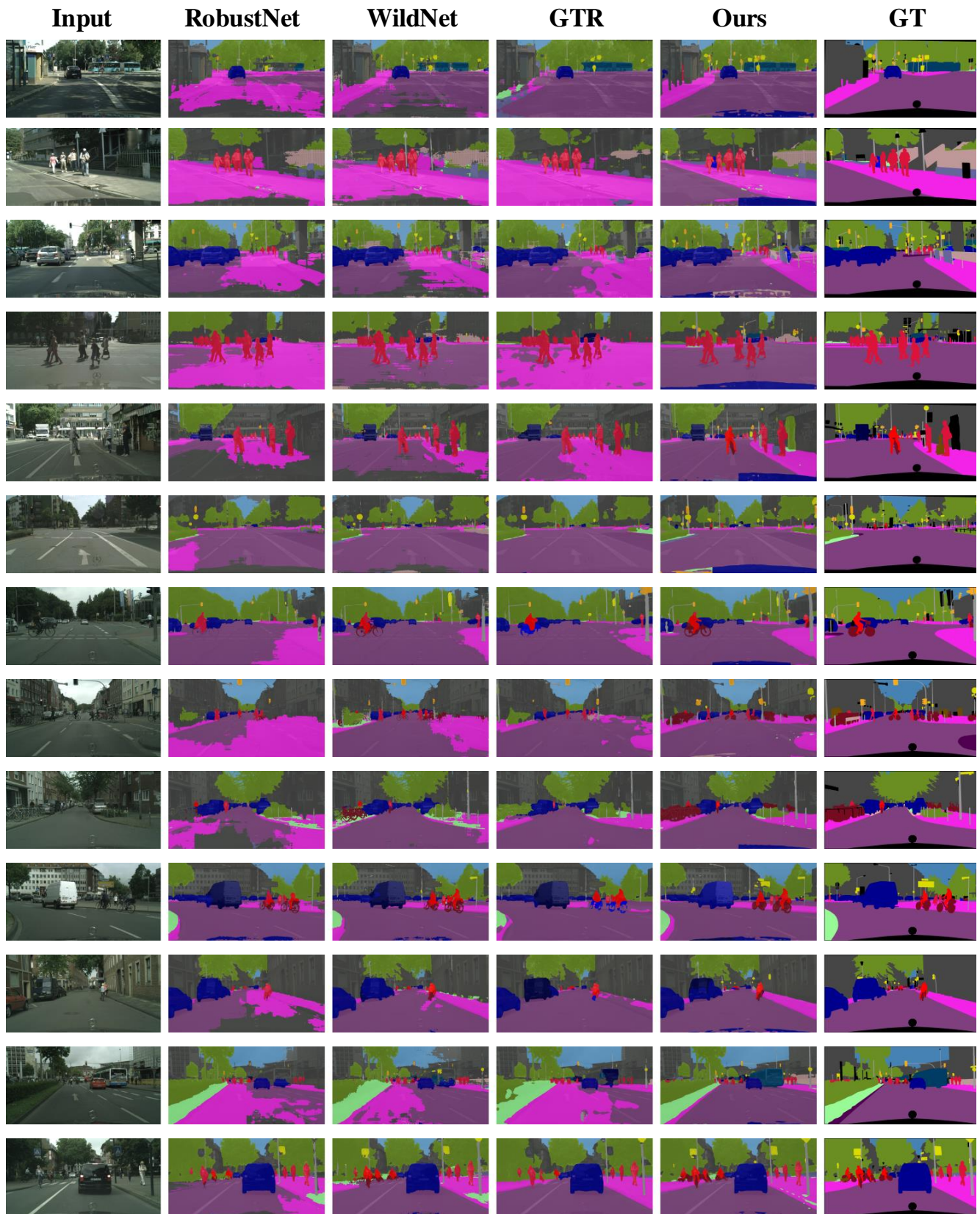


Figure 7. Prediction results of DINOv2+Rein on the Cityscapes validation set. The model is fine-tuned exclusively on the GTAV dataset, without access to any real-world urban-scene datasets.

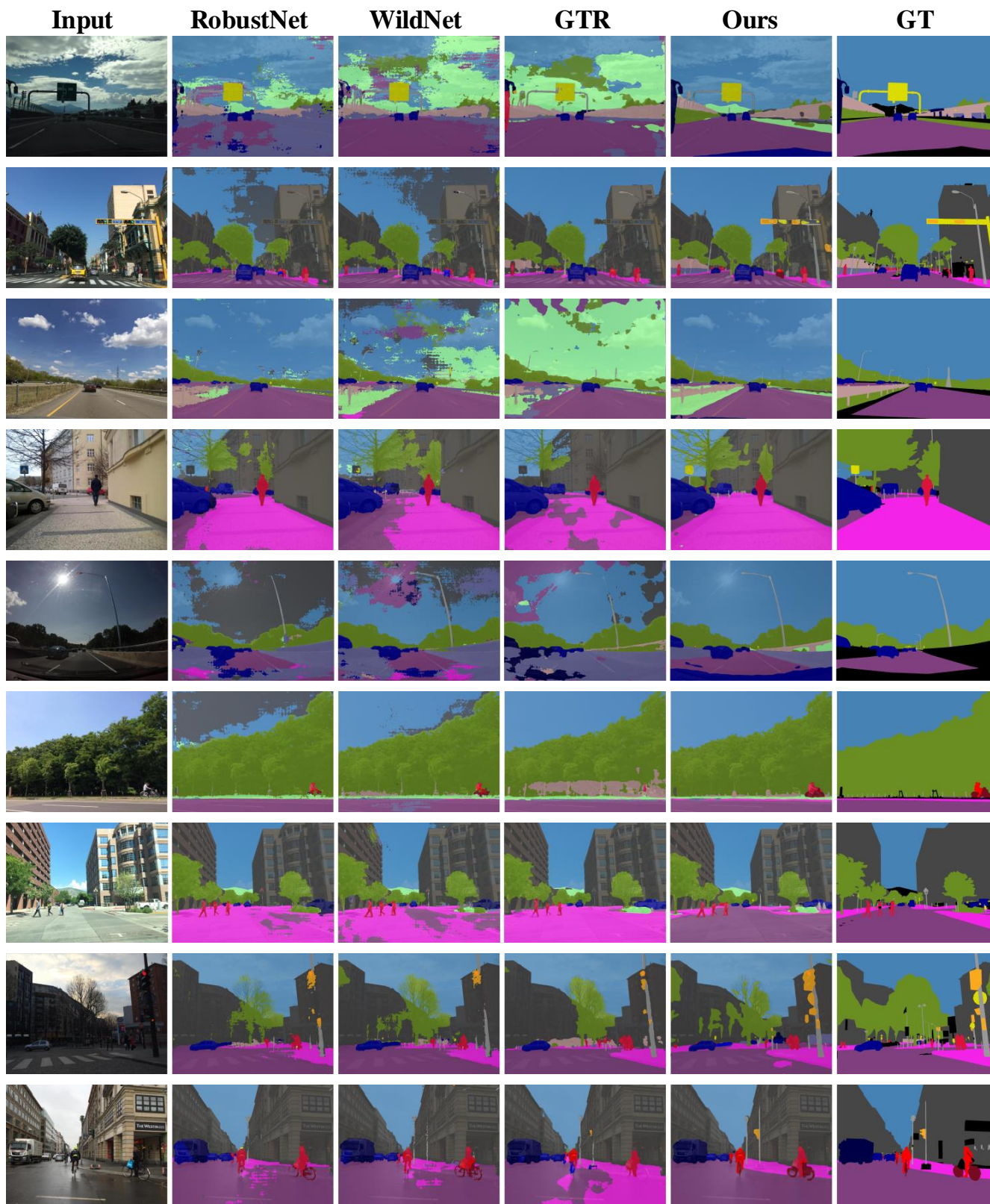


Figure 8. Prediction results of DINOv2+Rein on the Mapillary validation set. The model is fine-tuned exclusively on the GTAV dataset, without access to any real-world urban-scene datasets.

References

- [1] Yasser Benigmim, Subhankar Roy, Slim Essid, Vicky Kalogeiton, and Stéphane Lathuilière. Collaborating foundation models for domain generalized semantic segmentation, 2023. [7](#), [9](#)
- [2] Rishi Bommasani, Drew A. Hudson, Ehsan Adeli, Russ Altman, Simran Arora, Sydney von Arx, Michael S. Bernstein, Jeannette Bohg, Antoine Bosselut, Emma Brunskill, Erik Brynjolfsson, Shyamal Buch, Dallas Card, Rodrigo Castellon, Niladri Chatterji, Annie Chen, Kathleen Creel, Jared Quincy Davis, Dora Demszky, Chris Donahue, Moussa Doumbouya, Esin Durmus, Stefano Ermon, John Etchemendy, Kawin Ethayarajh, Li Fei-Fei, Chelsea Finn, Trevor Gale, Lauren Gillespie, Karan Goel, Noah Goodman, Shelby Grossman, Neel Guha, Tatsunori Hashimoto, Peter Henderson, John Hewitt, Daniel E. Ho, Jenny Hong, Kyle Hsu, Jing Huang, Thomas Icard, Saahil Jain, Dan Jurafsky, Pratyusha Kalluri, Siddharth Karamcheti, Geoff Keeling, Fereshhte Khani, Omar Khattab, Pang Wei Koh, Mark Krass, Ranjay Krishna, Rohith Kuditipudi, Ananya Kumar, Faisal Ladhak, Mina Lee, Tony Lee, Jure Leskovec, Isabelle Levent, Xiang Lisa Li, Xuechen Li, Tengyu Ma, Ali Malik, Christopher D. Manning, Suvir Mirchandani, Eric Mitchell, Zanele Munyikwa, Suraj Nair, Avanika Narayan, Deepak Narayanan, Ben Newman, Allen Nie, Juan Carlos Niebles, Hamed Nilforoshan, Julian Nyarko, Giray Ogut, Laurel Orr, Isabel Papadimitriou, Joon Sung Park, Chris Piech, Eva Portelance, Christopher Potts, Aditi Raghunathan, Rob Reich, Hongyu Ren, Frieda Rong, Yusuf Roohani, Camilo Ruiz, Jack Ryan, Christopher Ré, Dorsa Sadigh, Shiori Sagawa, Keshav Santhanam, Andy Shih, Krishnan Srinivasan, Alex Tamkin, Rohan Taori, Armin W. Thomas, Florian Tramèr, Rose E. Wang, William Wang, Bohan Wu, Jiajun Wu, Yuhuai Wu, Sang Michael Xie, Michihiro Yasunaga, Jiaxuan You, Matei Zaharia, Michael Zhang, Tianyi Zhang, Xikun Zhang, Yuhui Zhang, Lucia Zheng, Kaitlyn Zhou, and Percy Liang. On the opportunities and risks of foundation models, 2022. [3](#)
- [3] Nicolas Carion, Francisco Massa, Gabriel Synnaeve, Nicolas Usunier, Alexander Kirillov, and Sergey Zagoruyko. End-to-end object detection with transformers. In *European conference on computer vision*, pages 213–229. Springer, 2020. [5](#), [10](#)
- [4] Soravit Changpinyo, Piyush Sharma, Nan Ding, and Radu Soricut. Conceptual 12m: Pushing web-scale image-text pre-training to recognize long-tail visual concepts. In *Proceedings of the IEEE/CVF Conference on Computer Vision and Pattern Recognition*, pages 3558–3568, 2021. [11](#)
- [5] Prithvijit Chattopadhyay, Kartik Sarangmath, Vivek Vijaykumar, and Judy Hoffman. Pasta: Proportional amplitude spectrum training augmentation for syn-to-real domain generalization. In *Proceedings of the IEEE/CVF International Conference on Computer Vision*, pages 19288–19300, 2023. [1](#), [2](#), [3](#), [4](#), [6](#)
- [6] Lin Chen, Zhixiang Wei, Xin Jin, Huaian Chen, Miao Zheng, Kai Chen, and Yi Jin. Deliberated domain bridging for domain adaptive semantic segmentation. In *Advances in Neural Information Processing Systems*, pages 15105–15118. Curran Associates, Inc., 2022. [2](#)
- [7] Shoufa Chen, Chongjian Ge, Zhan Tong, Jiangliu Wang, Yibing Song, Jue Wang, and Ping Luo. Adaptformer: Adapting vision transformers for scalable visual recognition. *Advances in Neural Information Processing Systems*, 35:16664–16678, 2022. [2](#), [4](#), [6](#)
- [8] Bowen Cheng, Alex Schwing, and Alexander Kirillov. Per-pixel classification is not all you need for semantic segmentation. *Advances in Neural Information Processing Systems*, 34:17864–17875, 2021. [5](#), [10](#)
- [9] Bowen Cheng, Ishan Misra, Alexander G Schwing, Alexander Kirillov, and Rohit Girdhar. Masked-attention mask transformer for universal image segmentation. In *Proceedings of the IEEE/CVF conference on computer vision and pattern recognition*, pages 1290–1299, 2022. [2](#), [5](#), [6](#), [10](#)
- [10] Sungha Choi, Sanghun Jung, Huiwon Yun, Joanne T Kim, Seungryong Kim, and Jaegul Choo. Robustnet: Improving domain generalization in urban-scene segmentation via instance selective whitening. In *Proceedings of the IEEE/CVF Conference on Computer Vision and Pattern Recognition*, pages 11580–11590, 2021. [1](#), [3](#), [6](#), [10](#)
- [11] MMSegmentation Contributors. MMSegmentation: Openmmlab semantic segmentation toolbox and benchmark. <https://github.com/open-mmlab/mms Segmentation>, 2020. [6](#)
- [12] Marius Cordts, Mohamed Omran, Sebastian Ramos, Timo Rehfeld, Markus Enzweiler, Rodrigo Benenson, Uwe Franke, Stefan Roth, and Bernt Schiele. The cityscapes dataset for semantic urban scene understanding. In *Proceedings of the IEEE conference on computer vision and pattern recognition*, pages 3213–3223, 2016. [1](#), [2](#), [3](#), [5](#), [6](#)
- [13] Jia Deng, Wei Dong, Richard Socher, Li-Jia Li, Kai Li, and Li Fei-Fei. Imagenet: A large-scale hierarchical image database. In *2009 IEEE conference on computer vision and pattern recognition*, pages 248–255. Ieee, 2009. [2](#), [5](#), [9](#), [11](#)
- [14] Jian Ding, Nan Xue, Gui-Song Xia, Bernt Schiele, and Dengxin Dai. Hgformer: Hierarchical grouping transformer for domain generalized semantic segmentation. In *Proceedings of the IEEE/CVF Conference on Computer Vision and Pattern Recognition*, pages 15413–15423, 2023. [2](#), [6](#), [8](#)
- [15] Alexey Dosovitskiy, Lucas Beyer, Alexander Kolesnikov, Dirk Weissenborn, Xiaohua Zhai, Thomas Unterthiner, Mostafa Dehghani, Matthias Minderer, Georg Heigold, Sylvain Gelly, et al. An image is worth 16x16 words: Transformers for image recognition at scale. *arXiv preprint arXiv:2010.11929*, 2020. [3](#)
- [16] Mohammad Fahes, Tuan-Hung Vu, Andrei Bursuc, Patrick Pérez, and Raoul de Charette. A simple recipe for language-guided domain generalized segmentation. *arXiv preprint arXiv:2311.17922*, 2023. [4](#)
- [17] Qi Fan, Mattia Segu, Yu-Wing Tai, Fisher Yu, Chi-Keung Tang, Bernt Schiele, and Dengxin Dai. Towards robust object detection invariant to real-world domain shifts. In *The Eleventh International Conference on Learning Representations (ICLR 2023)*. OpenReview, 2023. [3](#)
- [18] Yuxin Fang, Quan Sun, Xinggang Wang, Tiejun Huang, Xinlong Wang, and Yue Cao. Eva-02: A visual representation

- for neon genesis. *arXiv preprint arXiv:2303.11331*, 2023. 1, 2, 3, 4, 6, 7, 8, 10, 11
- [19] Yuxin Fang, Wen Wang, Binhui Xie, Quan Sun, Ledell Wu, Xinggang Wang, Tiejun Huang, Xinlong Wang, and Yue Cao. Eva: Exploring the limits of masked visual representation learning at scale. In *Proceedings of the IEEE/CVF Conference on Computer Vision and Pattern Recognition*, pages 19358–19369, 2023. 1, 3, 4, 6, 7, 10
- [20] Ruoyu Feng, Jinming Liu, Xin Jin, Xiaohan Pan, Heming Sun, and Zhibo Chen. Prompt-icm: A unified framework towards image coding for machines with task-driven prompts. *arXiv preprint arXiv:2305.02578*, 2023. 4
- [21] Stuart Geman, Elie Bienenstock, and René Doursat. Neural networks and the bias/variance dilemma. *Neural computation*, 4(1):1–58, 1992. 9
- [22] Ziyang Gong, Fuhao Li, Yupeng Deng, Wenjun Shen, Xianzheng Ma, Zhenming Ji, and Nan Xia. Train one, generalize to all: Generalizable semantic segmentation from single-scene to all adverse scenes. In *Proceedings of the 31st ACM International Conference on Multimedia*, pages 2275–2284, 2023. 2
- [23] Ziyang Gong, Fuhao Li, Yupeng Deng, Deblina Bhattacharjee, Xiangwei Zhu, and Zhenming Ji. Coda: Instructive chain-of-domain adaptation with severity-aware visual prompt tuning, 2024. 2
- [24] Jose L. Gómez, Manuel Silva, Antonio Seoane, Agnès Borrás, Mario Noriega, Germán Ros, Jose A. Iglesias-Guitián, and Antonio M. López. All for one, and one for all: Urbansyn dataset, the third musketeer of synthetic driving scenes, 2023. 6, 9
- [25] Trevor Hastie, Robert Tibshirani, Jerome H Friedman, and Jerome H Friedman. *The elements of statistical learning: data mining, inference, and prediction*. Springer, 2009. 9
- [26] Kaiming He, Xiangyu Zhang, Shaoqing Ren, and Jian Sun. Deep residual learning for image recognition. In *Proceedings of the IEEE conference on computer vision and pattern recognition*, pages 770–778, 2016. 1, 2, 3, 8
- [27] Kaiming He, Xinlei Chen, Saining Xie, Yanghao Li, Piotr Dollár, and Ross Girshick. Masked autoencoders are scalable vision learners. In *Proceedings of the IEEE/CVF conference on computer vision and pattern recognition*, pages 16000–16009, 2022. 1, 2, 3, 6, 11
- [28] Neil Houlsby, Andrei Giurgiu, Stanislaw Jastrzebski, Bruna Morrone, Quentin De Laroussilhe, Andrea Gesmundo, Mona Attariyan, and Sylvain Gelly. Parameter-efficient transfer learning for nlp. In *International Conference on Machine Learning*, pages 2790–2799. PMLR, 2019. 2, 3
- [29] Edward J Hu, Yelong Shen, Phillip Wallis, Zeyuan Allen-Zhu, Yuanzhi Li, Shean Wang, Lu Wang, and Weizhu Chen. Lora: Low-rank adaptation of large language models. *arXiv preprint arXiv:2106.09685*, 2021. 2, 3, 4, 6, 8
- [30] Wei Huang, Chang Chen, Yong Li, Jiacheng Li, Cheng Li, Fenglong Song, Youliang Yan, and Zhiwei Xiong. Style projected clustering for domain generalized semantic segmentation. In *Proceedings of the IEEE/CVF Conference on Computer Vision and Pattern Recognition*, pages 3061–3071, 2023. 2, 6, 10
- [31] Menglin Jia, Luming Tang, Bor-Chun Chen, Claire Cardie, Serge Belongie, Bharath Hariharan, and Ser-Nam Lim. Visual prompt tuning. In *European Conference on Computer Vision*, pages 709–727. Springer, 2022. 2, 4, 6
- [32] Xueying Jiang, Jiaxing Huang, Sheng Jin, and Shijian Lu. Domain generalization via balancing training difficulty and model capability. In *Proceedings of the IEEE/CVF International Conference on Computer Vision*, pages 18993–19003, 2023. 2
- [33] Mengmeng Jing, Xiantong Zhen, Jingjing Li, and Cees GM Snoek. Order-preserving consistency regularization for domain adaptation and generalization. In *Proceedings of the IEEE/CVF International Conference on Computer Vision*, pages 18916–18927, 2023.
- [34] Christoph Kamann and Carsten Rother. Increasing the robustness of semantic segmentation models with painting-by-numbers. In *European Conference on Computer Vision*, pages 369–387. Springer, 2020. 2
- [35] Juwon Kang, Sohyun Lee, Namyup Kim, and Suha Kwak. Style neophile: Constantly seeking novel styles for domain generalization. In *Proceedings of the IEEE/CVF Conference on Computer Vision and Pattern Recognition*, pages 7130–7140, 2022. 1
- [36] Jared Kaplan, Sam McCandlish, Tom Henighan, Tom B Brown, Benjamin Chess, Rewon Child, Scott Gray, Alec Radford, Jeffrey Wu, and Dario Amodei. Scaling laws for neural language models. *arXiv preprint arXiv:2001.08361*, 2020. 2, 9
- [37] Hyeonseong Kim, Yoonsu Kang, Changgyoon Oh, and Kuk-Jin Yoon. Single domain generalization for lidar semantic segmentation. In *Proceedings of the IEEE/CVF Conference on Computer Vision and Pattern Recognition*, pages 17587–17598, 2023. 1
- [38] Jin Kim, Jiyoung Lee, Jungin Park, Dongbo Min, and Kwanghoon Sohn. Pin the memory: Learning to generalize semantic segmentation. In *Proceedings of the IEEE/CVF Conference on Computer Vision and Pattern Recognition*, pages 4350–4360, 2022. 2, 6, 10
- [39] Namyup Kim, Taeyoung Son, Jaehyun Park, Cuiling Lan, Wenjun Zeng, and Suha Kwak. Wedge: web-image assisted domain generalization for semantic segmentation. In *2023 IEEE International Conference on Robotics and Automation (ICRA)*, pages 9281–9288. IEEE, 2023. 1
- [40] Sunghwan Kim, Dae-hwan Kim, and Hoseong Kim. Texture learning domain randomization for domain generalized segmentation. In *Proceedings of the IEEE/CVF International Conference on Computer Vision (ICCV)*, pages 677–687, 2023. 2
- [41] Alexander Kirillov, Ross Girshick, Kaiming He, and Piotr Dollár. Panoptic feature pyramid networks. In *Proceedings of the IEEE/CVF conference on computer vision and pattern recognition*, pages 6399–6408, 2019. 10
- [42] Alexander Kirillov, Eric Mintun, Nikhila Ravi, Hanzi Mao, Chloe Rolland, Laura Gustafson, Tete Xiao, Spencer Whitehead, Alexander C. Berg, Wan-Yen Lo, Piotr Dollar, and Ross Girshick. Segment anything. In *Proceedings of the IEEE/CVF International Conference on Computer Vision (ICCV)*, pages 4015–4026, 2023. 1, 2, 3, 6, 11

- [43] Ananya Kumar, Aditi Raghunathan, Robbie Jones, Tengyu Ma, and Percy Liang. Fine-tuning can distort pretrained features and underperform out-of-distribution. *arXiv preprint arXiv:2202.10054*, 2022. 4
- [44] Alina Kuznetsova, Hassan Rom, Neil Alldrin, Jasper Uijlings, Ivan Krasin, Jordi Pont-Tuset, Shahab Kamali, Stefan Popov, Matteo Mallocci, Alexander Kolesnikov, et al. The open images dataset v4: Unified image classification, object detection, and visual relationship detection at scale. *International Journal of Computer Vision*, 128(7):1956–1981, 2020. 11
- [45] Suhyeon Lee, Hongje Seong, Seongwon Lee, and Euntai Kim. Wildnet: Learning domain generalized semantic segmentation from the wild. In *Proceedings of the IEEE/CVF Conference on Computer Vision and Pattern Recognition*, pages 9936–9946, 2022. 2, 3, 6, 8, 10
- [46] Brian Lester, Rami Al-Rfou, and Noah Constant. The power of scale for parameter-efficient prompt tuning. *arXiv preprint arXiv:2104.08691*, 2021. 2, 3
- [47] Feng Li, Hao Zhang, Huaizhe Xu, Shilong Liu, Lei Zhang, Lionel M. Ni, and Heung-Yeung Shum. Mask dino: Towards a unified transformer-based framework for object detection and segmentation. In *Proceedings of the IEEE/CVF Conference on Computer Vision and Pattern Recognition (CVPR)*, pages 3041–3050, 2023. 10
- [48] Fuhao Li, Ziyang Gong, Yupeng Deng, Xianzheng Ma, Renrui Zhang, Zhenming Ji, Xiangwei Zhu, and Hong Zhang. Parsing all adverse scenes: Severity-aware semantic segmentation with mask-enhanced cross-domain consistency. In *Proceedings of the AAAI Conference on Artificial Intelligence*, pages 13483–13491, 2024. 2
- [49] Xiang Lisa Li and Percy Liang. Prefix-tuning: Optimizing continuous prompts for generation. *arXiv preprint arXiv:2101.00190*, 2021. 2
- [50] Tsung-Yi Lin, Michael Maire, Serge Belongie, James Hays, Pietro Perona, Deva Ramanan, Piotr Dollár, and C Lawrence Zitnick. Microsoft coco: Common objects in context. In *Computer Vision—ECCV 2014: 13th European Conference, Zurich, Switzerland, September 6–12, 2014, Proceedings, Part V 13*, pages 740–755. Springer, 2014. 11
- [51] Xiao Liu, Kaixuan Ji, Yicheng Fu, Weng Tam, Zhengxiao Du, Zhilin Yang, and Jie Tang. P-tuning: Prompt tuning can be comparable to fine-tuning across scales and tasks. In *Proceedings of the 60th Annual Meeting of the Association for Computational Linguistics (Volume 2: Short Papers)*, pages 61–68, 2022. 2
- [52] Ze Liu, Yutong Lin, Yue Cao, Han Hu, Yixuan Wei, Zheng Zhang, Stephen Lin, and Baining Guo. Swin transformer: Hierarchical vision transformer using shifted windows. In *Proceedings of the IEEE/CVF international conference on computer vision*, pages 10012–10022, 2021. 3, 8
- [53] Ilya Loshchilov and Frank Hutter. Decoupled weight decay regularization. *arXiv preprint arXiv:1711.05101*, 2017. 6
- [54] Ningning Ma, Xiangyu Zhang, Hai-Tao Zheng, and Jian Sun. Shufflenet v2: Practical guidelines for efficient cnn architecture design. In *Proceedings of the European conference on computer vision (ECCV)*, pages 116–131, 2018. 3
- [55] Rodrigo Marcuzzi, Lucas Nunes, Louis Wiesmann, Jens Behley, and Cyrill Stachniss. Mask-based panoptic lidar segmentation for autonomous driving. *IEEE Robotics and Automation Letters*, 8(2):1141–1148, 2023. 10
- [56] Claudio Michaelis, Benjamin Mitzkus, Robert Geirhos, Evgenia Rusak, Oliver Bringmann, Alexander S Ecker, Matthias Bethge, and Wieland Brendel. Benchmarking robustness in object detection: Autonomous driving when winter is coming. *arXiv preprint arXiv:1907.07484*, 2019. 4
- [57] Gerhard Neuhold, Tobias Ollmann, Samuel Rota Buló, and Peter Kotschieder. The mapillary vistas dataset for semantic understanding of street scenes. In *Proceedings of the IEEE international conference on computer vision*, pages 4990–4999, 2017. 6
- [58] Maxime Oquab, Timothée Darcet, Théo Moutakanni, Huy Vo, Marc Szafraniec, Vasil Khalidov, Pierre Fernandez, Daniel Haziza, Francisco Massa, Alaaeldin El-Nouby, et al. Dinov2: Learning robust visual features without supervision. *arXiv preprint arXiv:2304.07193*, 2023. 1, 2, 3, 4, 6, 7, 8, 9, 10, 11
- [59] Xingang Pan, Ping Luo, Jianping Shi, and Xiaoou Tang. Two at once: Enhancing learning and generalization capacities via ibn-net. In *Proceedings of the European Conference on Computer Vision (ECCV)*, pages 464–479, 2018. 1, 3, 6, 8
- [60] Xingang Pan, Xiaohang Zhan, Jianping Shi, Xiaoou Tang, and Ping Luo. Switchable whitening for deep representation learning. In *Proceedings of the IEEE/CVF International Conference on Computer Vision*, pages 1863–1871, 2019. 3
- [61] Duo Peng, Yinjie Lei, Lingqiao Liu, Pingping Zhang, and Jun Liu. Global and local texture randomization for synthetic-to-real semantic segmentation. *IEEE Transactions on Image Processing*, 30:6594–6608, 2021. 1, 2, 3, 4, 6, 8
- [62] Duo Peng, Yinjie Lei, Munawar Hayat, Yulan Guo, and Wen Li. Semantic-aware domain generalized segmentation. In *Proceedings of the IEEE/CVF Conference on Computer Vision and Pattern Recognition*, pages 2594–2605, 2022. 2, 6, 8, 10
- [63] Alec Radford, Jong Wook Kim, Chris Hallacy, Aditya Ramesh, Gabriel Goh, Sandhini Agarwal, Girish Sastry, Amanda Askell, Pamela Mishkin, Jack Clark, et al. Learning transferable visual models from natural language supervision. In *International conference on machine learning*, pages 8748–8763. PMLR, 2021. 1, 2, 3, 6, 11
- [64] Nikhil Reddy, Abhinav Singhal, Abhishek Kumar, Mahsa Baktashmotlagh, and Chetan Arora. Master of all: Simultaneous generalization of urban-scene segmentation to all adverse weather conditions. In *European Conference on Computer Vision*, pages 51–69. Springer, 2022. 1
- [65] Stephan R Richter, Vibhav Vineet, Stefan Roth, and Vladlen Koltun. Playing for data: Ground truth from computer games. In *Computer Vision—ECCV 2016: 14th European Conference, Amsterdam, The Netherlands, October 11–14, 2016, Proceedings, Part II 14*, pages 102–118. Springer, 2016. 1, 2, 3, 5, 6
- [66] German Ros, Laura Sellart, Joanna Materzynska, David Vazquez, and Antonio M. Lopez. The synthia dataset: A large collection of synthetic images for semantic segmenta-

- tion of urban scenes. In *The IEEE Conference on Computer Vision and Pattern Recognition (CVPR)*, 2016. 6
- [67] Christos Sakaridis, Dengxin Dai, and Luc Van Gool. Acdc: The adverse conditions dataset with correspondences for semantic driving scene understanding. In *Proceedings of the IEEE/CVF International Conference on Computer Vision*, pages 10765–10775, 2021. 4
- [68] Mark Sandler, Andrew Howard, Menglong Zhu, Andrey Zhmoginov, and Liang-Chieh Chen. Mobilenetv2: Inverted residuals and linear bottlenecks. In *Proceedings of the IEEE conference on computer vision and pattern recognition*, pages 4510–4520, 2018. 1, 2, 3
- [69] Shuai Shao, Zeming Li, Tianyuan Zhang, Chao Peng, Gang Yu, Xiangyu Zhang, Jing Li, and Jian Sun. Objects365: A large-scale, high-quality dataset for object detection. In *Proceedings of the IEEE/CVF international conference on computer vision*, pages 8430–8439, 2019. 11
- [70] Piyush Sharma, Nan Ding, Sebastian Goodman, and Radu Soricut. Conceptual captions: A cleaned, hypernymed, image alt-text dataset for automatic image captioning. In *Proceedings of the 56th Annual Meeting of the Association for Computational Linguistics (Volume 1: Long Papers)*, pages 2556–2565, 2018. 11
- [71] Karen Simonyan and Andrew Zisserman. Very deep convolutional networks for large-scale image recognition. *arXiv preprint arXiv:1409.1556*, 2014. 1, 3
- [72] Zhiqiang Tang, Yunhe Gao, Yi Zhu, Zhi Zhang, Mu Li, and Dimitris N. Metaxas. Crossnorm and selfnorm for generalization under distribution shifts. In *Proceedings of the IEEE/CVF International Conference on Computer Vision (ICCV)*, pages 52–61, 2021. 1, 2
- [73] Jan-Aike Termöhlen, Timo Bartels, and Tim Fingscheidt. A re-parameterized vision transformer (revt) for domain-generalized semantic segmentation. In *Proceedings of the IEEE/CVF International Conference on Computer Vision*, pages 4376–4385, 2023. 1
- [74] Wei Wang, Zhun Zhong, Weijie Wang, Xi Chen, Charles Ling, Boyu Wang, and Nicu Sebe. Dynamically instance-guided adaptation: A backward-free approach for test-time domain adaptive semantic segmentation. In *Proceedings of the IEEE/CVF Conference on Computer Vision and Pattern Recognition*, pages 24090–24099, 2023. 6, 10
- [75] Zhixiang Wei, Lin Chen, Tao Tu, Pengyang Ling, Huaian Chen, and Yi Jin. Disentangle then parse: Night-time semantic segmentation with illumination disentanglement. In *Proceedings of the IEEE/CVF International Conference on Computer Vision (ICCV)*, pages 21593–21603, 2023. 2
- [76] Zhenyao Wu, Xinyi Wu, Xiaoping Zhang, Lili Ju, and Song Wang. Siamdoge: Domain generalizable semantic segmentation using siamese network. In *European Conference on Computer Vision*, pages 603–620. Springer, 2022. 1
- [77] Qi Xu, Liang Yao, Zhengkai Jiang, Guannan Jiang, Wenqing Chu, Wenhui Han, Wei Zhang, Chengjie Wang, and Ying Tai. Dirl: Domain-invariant representation learning for generalizable semantic segmentation. In *Proceedings of the AAAI Conference on Artificial Intelligence*, pages 2884–2892, 2022. 1, 2
- [78] Fisher Yu, Haofeng Chen, Xin Wang, Wenqi Xian, Yingying Chen, Fangchen Liu, Vashisht Madhavan, and Trevor Darrell. Bdd100k: A diverse driving dataset for heterogeneous multitask learning. In *Proceedings of the IEEE/CVF conference on computer vision and pattern recognition*, pages 2636–2645, 2020. 6
- [79] Xiangyu Yue, Yang Zhang, Sicheng Zhao, Alberto Sangiovanni-Vincentelli, Kurt Keutzer, and Boqing Gong. Domain randomization and pyramid consistency: Simulation-to-real generalization without accessing target domain data. In *Proceedings of the IEEE/CVF International Conference on Computer Vision*, pages 2100–2110, 2019. 6, 8
- [80] Elad Ben Zaken, Shauli Ravfogel, and Yoav Goldberg. Bitfit: Simple parameter-efficient fine-tuning for transformer-based masked language-models. *arXiv preprint arXiv:2106.10199*, 2021. 2, 3
- [81] Bowen Zhang, Zhi Tian, Quan Tang, Xiangxiang Chu, Xiaolin Wei, Chunhua Shen, et al. Segvit: Semantic segmentation with plain vision transformers. *Advances in Neural Information Processing Systems*, 35:4971–4982, 2022. 5, 10
- [82] Yuhang Zhang, Shishun Tian, Muxin Liao, Guoguang Hua, Wenbin Zou, and Chen Xu. Learning shape-invariant representation for generalizable semantic segmentation. *IEEE Transactions on Image Processing*, 2023. 1
- [83] Zhun Zhong, Yuyang Zhao, Gim Hee Lee, and Nicu Sebe. Adversarial style augmentation for domain generalized urban-scene segmentation. *Advances in Neural Information Processing Systems*, 35:338–350, 2022. 1, 2, 3, 4, 6
- [84] Bolei Zhou, Hang Zhao, Xavier Puig, Tete Xiao, Sanja Fidler, Adela Barriuso, and Antonio Torralba. Semantic understanding of scenes through the ade20k dataset. *International Journal of Computer Vision*, 127:302–321, 2019. 11
- [85] Kaiyang Zhou, Jingkang Yang, Chen Change Loy, and Ziwei Liu. Learning to prompt for vision-language models. *International Journal of Computer Vision*, 130(9):2337–2348, 2022. 2